

Stable isotope systematics of two cenotes from the northern Yucatan Peninsula, Mexico

Richard A. Socki¹

Lockheed Martin, Astromaterials Research and Exploration Science, Mail Code C-23, 2400 NASA Road, Houston, Texas 77058.

Eugene C. Perry, Jr.

Northern Illinois University, Department of Geology and Environmental Sciences, DeKalb, Illinois 60115.

Christopher S. Romanek

University of Georgia, Savannah River Ecology Lab, Aiken, South Carolina 29802.

Abstract

Deep water-filled sinkholes, cenotes, are common in the northern Yucatan Peninsula. At least five of these cenotes are deep enough to extend through a freshwater lens of meteoric origin in which $\delta^{18}\text{O}$ and δD follow the trend $\delta\text{D} = 8.11 \times \delta^{18}\text{O} + 10.4$. Below this freshwater lies saline water that originated as seawater and has retained its seawater isotopic identity. Deep cenotes, characterized by input of variable amounts of organic debris from tropical vegetation and by poor circulation below the fresh-/saltwater interface, provide excellent water columns in which to study sulfur redox phenomena. Measurements include O, H, and S isotope composition, conductivity, sulfur speciation, and pH from two cenotes (Ucil, 98 m deep, and Xcolac, 125 m deep). Strong ^{34}S enrichment of sulfate and ^{34}S depletion of sulfide indicate anaerobic bacterial reduction of sulfate. A shift in the isotopic composition of sulfur in Xcolac from a seawater value of +21.0‰ (CDT) to +41.8‰ indicates conversion of sulfate to isotopically light sulfide. Mass balance calculations indicate that escape of isotopically light sulfur from the system is a slow process. At 80 m in Xcolac, a difference in sulfur isotope composition between sulfate and sulfide ($\Delta^{34}\text{S}$) of 63.2‰ is observed and could be the result of multiple sulfate reduction reactions. Higher in the water column, sulfide oxidation occurs, probably the result of bacterially mediated sulfide oxidation processes. A deep observation well (lacking organic matter input) shows only a slight deviation in sulfur isotope composition of sulfate from seawater values.

We report here the relations between depth and the parameters O, H, and S isotopic composition; conductivity; sulfur speciation; and pH of two deep, water-filled karst sinkholes (known locally as cenotes from the indigenous Maya word *tzonot* = lake) in the north-central Yucatan of Mexico. These cenotes, Xcolac and Ucil, both extend through the regional freshwater lens into an extensive saltwater intrusion containing water isotopically indistinguishable (H, O, and S) from local seawater. Although they are not the deepest cenotes in northern Yucatan (Andreas W. Matthes describes a 168-m-deep cenote, Sabak-Ha, unpubl.), they are the most accessible deep cenotes that can be sampled conveniently from the surface.

Ucil and Xcolac Cenotes offer an unusual, perhaps unique, opportunity to study bacterially mediated redox reactions between sulfur- and carbon-bearing components in natural low-temperature aqueous systems. Whereas elsewhere such redox reactions commonly take place within a sediment column over a depth range of a few centimeters or in water columns that experience strong seasonal changes, in the Yucatan, cenote redox processes are spread through meters of

a stratified, stable water column. Three factors make redox processes extremely important in the geochemistry of these cenotes: (1) density stratification that prevents turnover in the lower part of the system, (2) high concentration of sulfur species (that enter the system as sulfate) in the lower water layer (modified seawater), and (3) extensive tropical vegetation, which is trapped in cone-shaped depressions surrounding the cenotes and which falls into the cenotes to provide a rich source of carbon and trace nutrients for bacterial growth. Socki (1984) examined the chemistry of deep cenotes in northwestern Yucatan, Mexico. Stoessell et al. (1993) have described sulfate reduction and sulfide oxidation occurring in deep cenotes located in Quintana Roo along the eastern coast of the Yucatan Peninsula. One or more of the following characteristics distinguish deep cenotes from other aqueous environments of sulfate reduction such as fjords (Fossing and Jorgensen 1990) and marine caverns (Bottrell et al. 1991): (1) regeneration of the saltwater column from the permeable aquifer system at the sides of the cenotes, (2) carbonate host environment, (3) lack of significant sediment at the bottom of the water column, (4) absence of base metal ions for metal sulfide precipitation, and (5) abundant vegetation and relatively high water temperature that are functions of the tropical environment.

Sulfate of the saline intrusion in both cenotes is strongly enriched in ^{34}S relative to seawater sulfate because of the action of sulfate-reducing bacteria. A difference in sulfur isotopic composition between sulfate and sulfide ($\Delta^{34}\text{S} \leq$

¹ Corresponding author (rsocki@ems.jsc.nasa.gov).

Acknowledgments

We acknowledge Jaime Durazo, Miguel Villasuso, and Salvador Gaona for help with field work associated with this study. A previous version of this manuscript was reviewed by Hazel Barton and Pat Shanks and two anonymous reviewers.

63.2‰) is observed at a depth of 80 m in Xcolac Cenote and is consistent with this interpretation. This large sulfur isotope fractionation coupled with cycling between sulfate reduction and sulfide oxidation might indicate bacterial sulfur disproportionation (as discussed by Canfield et al. 1998; Habicht et al. 1998; Canfield 2001). In contrast with sulfur isotope data from the cenotes, data from a deep (180 m) observation well show that there is little variation in sulfur isotope composition as a function of depth. Both sulfur isotope and pH data indicate that specific processes occur within specific and sometimes narrow depth intervals.

Materials and methods

Description of study area—The Yucatan Peninsula is a low-lying karst platform whose near-surface rocks are porous, highly permeable Tertiary limestones and dolomites (Weidie 1985). The upper 96 m of a core taken at Cenotillo (within 2 km of Ucil Cenote and 32 km from Xcolac Cenote) is composed of limestone consisting of 83% or more of calcite with no more than a trace of dolomite (Gmitro 1986). Dolomite is abundant in this core between 96 m and the bottom of the hole at 100 m. The water table at the Cenotillo borehole is 20 m below the surface. Thus, making the quite reasonable assumption of horizontal strata, this core could be representative of the upper 80 m of the geologic section lying below the water table at Ucil. It is significant that no aquitard layers were encountered in the Cenotillo core and are, in fact, rare throughout the northern Yucatan peninsula (Perry et al. 1995).

Xcolac and Ucil Cenotes lie at the outer margin of a semi-circular zone (Ring of Cenotes) characterized by an anomalously high abundance of cenotes, the result of enhanced permeability (Perry et al. 1995). According to Perry et al. (1995) enhanced permeability could result from a set of fractures associated with subsidence of the Chicxulub (K/T) Impact Crater centered about 30 km NE of Merida (Hildebrand et al. 1991; Sharpton et al. 1993). Furthermore, it is probable that a layer of K/T boundary breccia containing fragments ejected from the Chicxulub Impact Crater (Sharpton et al. 1993; Ward et al. 1995) is present beneath Ucil and Xcolac. This breccia contains gypsum and other highly soluble evaporite minerals, and dissolution of these minerals during periods of low sea stand could contribute to the development of deep cenotes (Perry et al. in press).

The essential hydrogeology of the north-central Yucatan can be summarized as follows: meteoric precipitation (~ 1.0 m yr⁻¹) falls on the tropical peninsula and infiltrates quickly into porous, permeable carbonate rock. This less-dense, fresh groundwater “floats” on a saline wedge of groundwater derived from seawater. The interface between the upper and lower groundwater bodies is a zone of mixing between the two end members (Back and Hanshaw 1978; Stoessell et al. 1993). Regional water table measurements (Marin 1990) show that the elevation of the water table in northwest Yucatan is very regular and almost flat, with a seasonal variation of about 1 m. Overall aquifer characteristics indicate high permeability both through large conduits (cavern permeability) and on a finer scale (moldic permeability). Al-

though the relationship is complicated by slight seasonal variations in the elevation of the water table, depth to the interface between fresh and salt water is closely related to elevation of the water table above mean sea level (Perry et al. 1989). Inland from the coast, this depth follows the prediction of the Ghyben–Herzberg relation (discussed by Freeze and Cherry 1979).

Ucil and Xcolac Cenotes are similar in many respects. They are distinguished by their different geometries. Approximate physical profiles of both cenotes are shown in Fig. 1. Xcolac (located about 55 km south of the Gulf of Mexico) lies in a funnel-shaped karst depression. It has a surface diameter of about 70 m and a depth of about 125 m (as measured by soundings). Lake level, which corresponds to the local water table, is about 20 m beneath the general land elevation. Ucil, which is 50 km from the sea and 98 m deep (by soundings), is only about 10 m in diameter at the water surface but widens somewhat a few meters beneath the water surface. It receives less light and less falling organic matter than Xcolac because it is sheltered within a subaerial cave with a partly collapsed roof. In addition, residence time of groundwater is less in the water column of Ucil, assuming that groundwater flow velocities are similar in both cenotes. The combined effect of less light, lower organic input, and short residence time is less pronounced variation in both pH and sulfur isotope composition in Ucil.

Observation well and freshwater wells—Characteristics of fresh groundwater in northern Yucatan are described by Perry et al. (in press). In the vicinity of Xcolac and Ucil Cenotes, this is dilute water in equilibrium with calcite and dolomite and contains a slight admixture of seawater from the underlying saline intrusion. In addition to water from cenotes, water samples were taken from three wells near Merida, Yucatan (Fig. 1) to compare with water samples from the cenotes. Shallow samples came from two wells chosen from a field of 22 wells operated by Junta de Agua Potable y Alcantarillado de Yucatan (JAPY). These are shallow wells (depth below the water table is 10 to 20 m) that are pumped continuously to supply (potable) water to Merida. Samples were taken by opening a valve at the wellhead. A deep (180 m) injection/observation well, Pozo de Absorción (PD-II), located a few kilometers northwest of Merida, was also sampled to provide background data.

Sampling and analytical procedures—Field sampling: Field measurements of the water column, which included depth (determined by a pressure sensor) and conductivity, were taken using a probe specific to these parameters. pH measurements and additional conductivity measurements were made with a different, more precise probe (Datasonde 3) to a maximum depth of 95 m. Water samples were collected using a Nansen-type sampling bottle attached to a graduated nylon rope. The sampler was lowered slowly to a desired depth and held at that depth for at least 1 min, allowing the system to approach thermal stability. Then a brass weight (messenger) was attached to the rope and allowed to fall, triggering the closing mechanism on the sampler. Once collected, all water was immediately passed through 0.45- μ m membrane filters to remove bacteria and thus to mini-

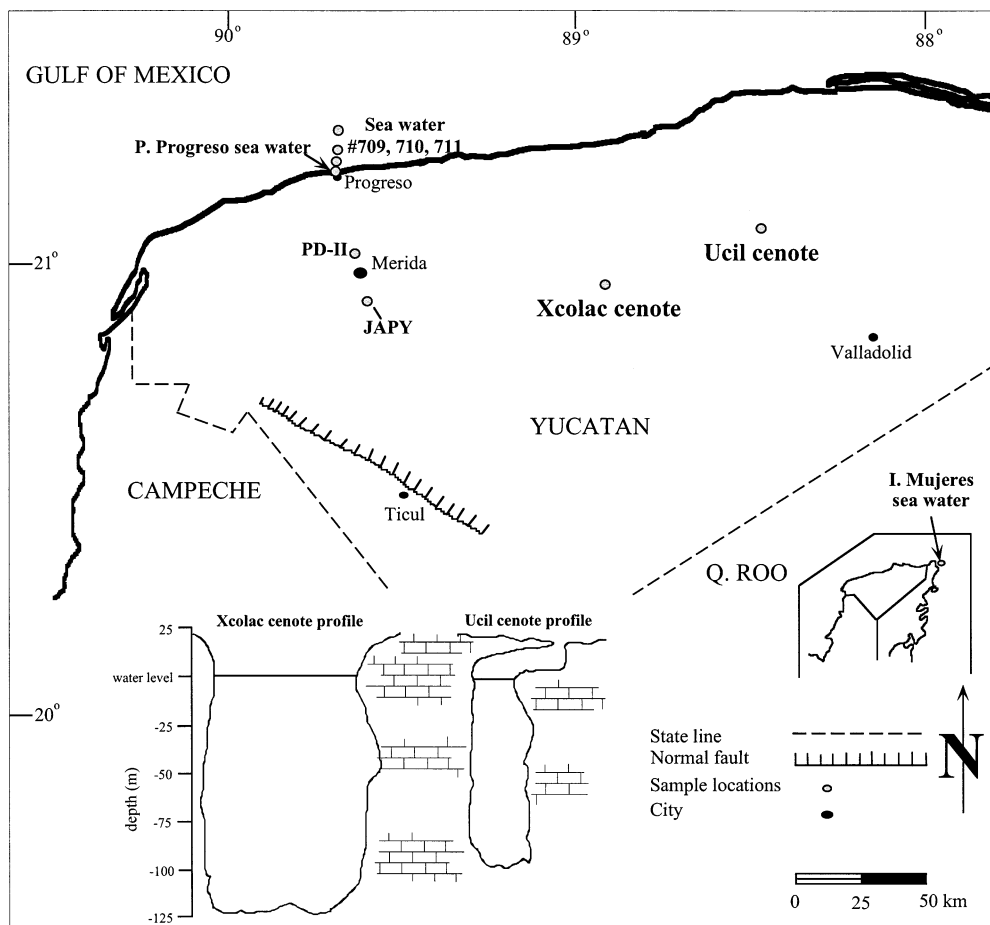


Fig. 1. Map of the northern Yucatan Peninsula, Mexico, showing both sample locations and approximate cenote profiles.

mize bacterially mediated redox reactions. Water samples from the saline wedge that were collected for analysis of $^{34}\text{S}/^{32}\text{S}$ in sulfate were treated in the field with 0.5 M BaCl_2 to precipitate BaSO_4 . In order to test the reliability of this technique, several seawater samples were treated in a similar manner in the laboratory. Samples treated in the laboratory had sulfur isotope values within $\pm 0.4\%$ of the isotopic composition of the accepted value for modern seawater (21.0‰). Saline water samples to be used for the determination of $^{34}\text{S}/^{32}\text{S}$ in sulfide were treated in the field with a large excess of 0.1 M AgNO_3 , thus precipitating Ag_2S . In order to dissolve AgCl that was also precipitated by this treatment, samples were subsequently treated with concentrated NH_4OH . HS^- , H_2S , and perhaps polysulfide all are precipitated as Ag_2S by our collection procedure. Although our sampling strategy fixed the isotopic composition of reduced sulfur under difficult field sampling conditions, it does not distinguish between the distinct reduced species present.

Laboratory extractions: Samples to be used for analyses of $^{18}\text{O}/^{16}\text{O}$ and H/D from water were stored in 100-liter glass bottles and sealed to protect against evaporation. Oxygen isotopic composition of these waters was determined by the CO_2 equilibration technique of Epstein and Mayeda (1953).

Sample reproducibility using this technique was generally better than $\pm 0.05\%$.

Hydrogen isotopes were extracted by passing 5 to 10 μl of water over a 550°C furnace containing uranium powder. In addition to our laboratory working standards, we analyzed three international water standards, V-SMOW, GISP, and SLAP, whose isotopic composition is reported by Hut (1987). Overall hydrogen isotope reproducibility was $\pm 1.5\%$.

Water samples taken from above the fresh-/saltwater interface contained dissolved sulfate in low concentrations. After filtration, samples were carried to the laboratory where they were passed through an ion exchange column containing Biorad #5A ion exchange resin. Sulfate was then leached from the resin by passing 100 ml of 0.5 M NaCl solution through the column. The resulting solution was treated with concentrated HCl to pH 2.0, and the solution was boiled for 10 min to expel any carbonate that might be present. BaCl_2 (0.5 M) was then added to precipitate BaSO_4 , which was oven-dried overnight.

For sulfur isotope analysis, barium sulfate was ground to a fine powder, packed with quartz wool into 8-mm (o.d.) quartz capsules, placed in the bottom of a 12-mm (o.d.) quartz tube, and heated under vacuum by a soft flame. After

degassing, the sample and tube were heated to just above the melting point of quartz, producing SO_2 gas for isotopic analysis following the procedure of Holt and Engelkemeir (1970). There is no direct way to measure yields using this method, but routine analyses of our laboratory barium sulfate standard (Elgin Barite), which has been calibrated to the CDT (Canyon Diablo Troilite scale), show reproducibility of $\pm 0.4\%$.

Analyses—All analyses of SO_2 , H_2 , and CO_2 gases prepared from samples were made on a Varian MAT 250 isotope ratio mass spectrometer equipped with a hydrogen collector. All oxygen and hydrogen data are reported relative to SMOW (standard mean ocean water Craig 1957). Composition estimates of sulfate and sulfide are based on weighing of precipitates collected in the field and have a precision of about $\pm 10\%$ because they were precipitated in uncalibrated 1.0-liter containers. The collection strategy was designed to fix the in-situ sulfur isotope composition, rather than to quantify concentration of sulfate and sulfide. Nevertheless, because of large excesses of BaCl_2 and AgNO_3 used, sulfate and sulfide precipitated quantitatively during the treatment, and the results are sufficiently precise for approximate mass balance calculations.

Results and discussion

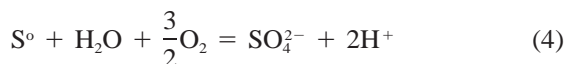
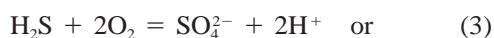
Sulfate concentration, sulfide concentration, and pH are related in a complex way in Xcolac and Ucil. Principal redox reactants in these two water columns are sulfate, which enters from within the aquifer as a component of the saline lens; organic carbon, which enters as decaying tropical vegetation from the respective drainage basins; and oxygen from the surface (and possibly from mildly oxygenated seawater entering from the sides of the cenotes). Tropical vegetation falls into the cenote at the surface and consists mostly of solid fragments of leaves and branches, which eventually become waterlogged and sink to the bottom. The process of bacterially mediated sulfate reduction, observed in Bahamian blue holes by Bottrell et al. (1991), produces either hydrogen sulfide



or elemental sulfur.



Much of the organic matter that does not react in the upper, oxidized layers of the respective water columns eventually sinks and is available for redox reactions in the lower saline layer. Furthermore, acidity is generated where oxidation of reduced sulfur species occurs as follows.



H_2S has a pK_1 of 6.9 and as such, within the pH range of Xcolac, will partially dissociate to form H^+ and HS^- . Sulfate reduction occurring at both the mixing zone and at the bottom of the cenotes generates HCO_3^- alkalinity (Eqs. 1, 2),

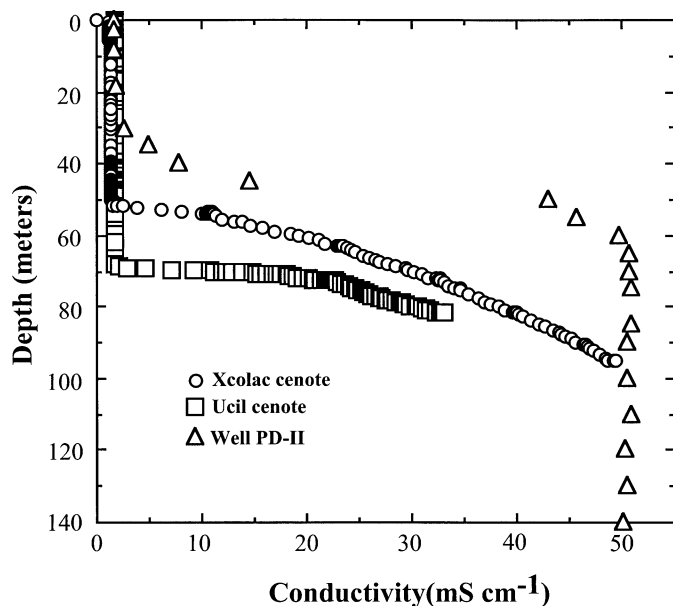


Fig. 2. Conductivity (mS) versus depth for water from Xcolac and Ucil Cenotes and well PD-II. Measurements in the well were taken using a conductivity-specific probe with a depth accuracy of ± 2.0 m, whereas measurements in the cenotes were taken using a Datasonde 3 probe with an accuracy of ± 0.2 m.

whereas oxidation is accompanied by hydrogen ion production. Thus, pH is a sensitive indicator of redox processes.

Water column depth profiles—For both Ucil and Xcolac Cenotes we discuss essential aspects of profiles of water depth versus conductivity, pH, concentration of sulfate, and isotopic composition of sulfur in sulfate and oxygen and deuterium in water. We include additional profiles of sulfide and sulfate concentration and isotopic composition of sulfur in sulfide and sulfate of Xcolac Cenote. For comparison, we present measurements of the isotopic composition of oxygen and deuterium in local seawater and sulfur in seawater sulfate and the depth profiles of the isotopic composition of oxygen in water and sulfur in sulfate of a local deep well. Subsequently, we interpret correlations among these parameters.

Note that water samples for chemical/isotopic analysis were obtained with a Nansen-type bottle attached to a nylon line with marked depths, whereas pH and conductivity measurements in Ucil and Xcolac (Figs. 2–4) were made with a Datasonde 3 instrument that determined depth by pressure measurements in a water column of variable density. The two sets of depth measurements can vary by as much as ± 2.0 m. This difference is significant only for interpretation of pH in the narrow zone between 51 and 54 m in Xcolac, shown in Fig. 4. The pH probe, which has a maximum operating depth of 100 m, was not lowered below the maximum depths indicated to avoid the risk of leaking seals (in Xcolac) and fouling on the hard bottom (in Ucil).

Conductivity: The conductivities (in mS cm^{-1}), which give a general indication of ion concentration, are plotted as a function of depth for Xcolac and Ucil Cenotes and Well

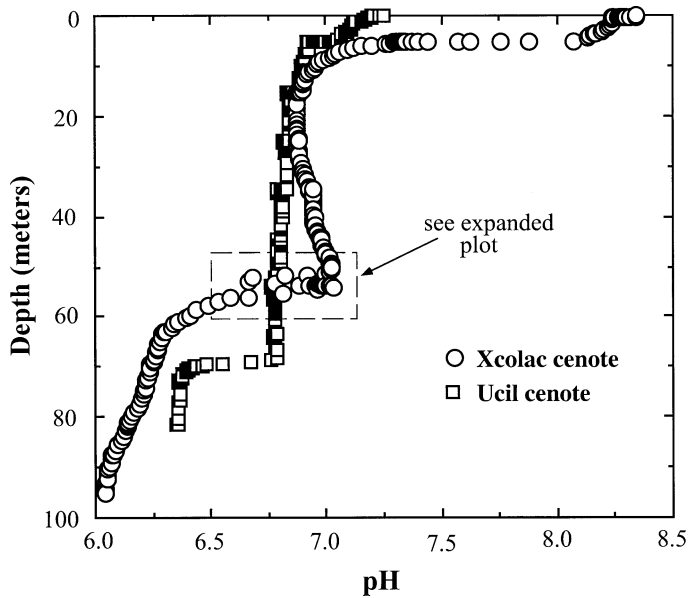


Fig. 3. pH versus depth from Xcolac and Ucil Cenotes. pH measurements were taken using a probe (Datasonde 3) with an accuracy of ± 0.2 m.

PD-II in Fig. 2. There is a sharp increase in conductivity of water below 52 m in Xcolac and 69 m in Ucil. With increasing depth, conductivity values of the waters from both Xcolac and Ucil approach the values of modern seawater (49.4 mS cm^{-1} at 95.2 m in Xcolac and 33.4 mS cm^{-1} at 80.5 m in Ucil). These cenote measurements are closely comparable to measurements of 1.4 mS cm^{-1} at 32 m and 50 mS cm^{-1} at 140 m made in the deep well PD-II near Merida. If we define the freshwater/saltwater interface as the surface where the conductivity is the mean between freshwater and seawater end members, the thickness of the freshwater lens is 52 m at Xcolac and 69 m at Ucil.

Conductivity gradients in the water columns of the two cenotes indicate an upward transfer of material, and differences in the conductivity versus depth profiles of each cenote (Fig. 2) reflect their distinctive water mixing patterns, which are related to geometric characteristics (primarily width) of the cenote, permeability of the aquifer rocks, and fluxes of material entering and leaving the water column. As already noted, flux of organic material into Xcolac is greater than that into Ucil. Assuming similar groundwater flow velocities, residence time (related to horizontal transfer distance) is several times longer in Xcolac than in Ucil.

pH: Xcolac water pH ranges from 8.3 at the surface to 6.0 at 95 m depth (Fig. 3). Two narrow zones with variations of 0.6 pH units occur just below the fresh-/saltwater interface (Fig. 4). The uppermost of these, which we have labeled the "sulfide oxidation zone," occurs at 53 m and is marked by a pH minimum characteristic of the reactions in Eqs. 3 and 4. Beneath this is a pH maximum at 54 m that indicates reduction (Eqs. 1, 2). The latter marks the upper boundary of what is labeled the "sulfate reduction zone."

The pH profile at Ucil is less complicated than the Xcolac profile. pH ranges from 7.2 at the surface to 6.4 at 81.5 m

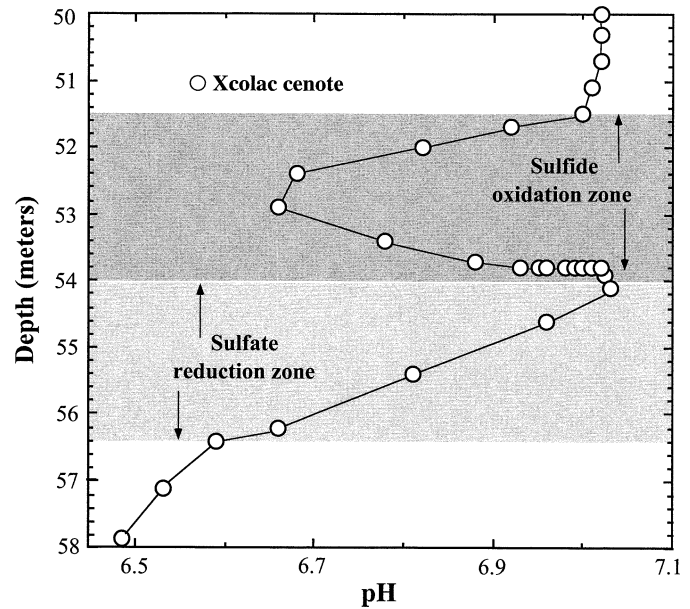


Fig. 4. Detailed pH versus depth near the fresh-/saltwater interface from Xcolac Cenote.

with a sharp break at ~ 69 m, corresponding to the fresh-/saltwater interface as shown by conductivity data (Fig. 2). Interpretation of low pH values within the deeper parts of the saline intrusion in each cenote (to pH 6.1 at the base of the measured water column at Xcolac and 6.4 at the base of Ucil) is more problematic. High sulfide concentrations and positive shifts in ^{34}S of sulfate from the seawater value (Figs. 7, 8) demonstrate that sulfide is forming in the lower water column and producing alkalinity in accordance with Eqs. 1 and 2. It is possible but unlikely that mildly oxidized water is entering the system at depth, leading to sulfide oxidation (Eq. 3) and that this, balanced against sulfide loss leads to a net reduction in pH. Also, carbonic acid ($\text{p}K_1 = 6.3$) is a weak acid, and a high $\text{CO}_{2(\text{aq})}$ concentration from respiration will lower the pH.

Another possible contributor to low pH at depth (cf. Stern et al. 2002) is the following reaction.



The probable source for this CaSO_4 is evaporite and impact breccia layers beneath the two cenotes. Such layers are widespread in subsurface rocks of the Yucatan Peninsula. Rebolledo-Viera et al. (2000), and Ward et al. (1995) reported them at depths of somewhat greater than 200 m in core from a nearby petroleum exploration well. The most direct evidence that CaSO_4 is dissolving in deep water entering at the base of the cenotes comes from exceptionally high concentrations of strontium (30 ppm) at the base of the water column in Ucil as reported by Gmitro (1986). Perry and Socki (unpubl. data) subsequently confirmed these high strontium concentrations, and Perry et al. (in press) used a peninsula-wide linear correlation ($r^2 = 0.91$) between strontium and sulfate ion to suggest that the high strontium content of deep Ucil water comes from deep circulation of groundwater into evaporite layers beneath the accessible floors of Ucil and

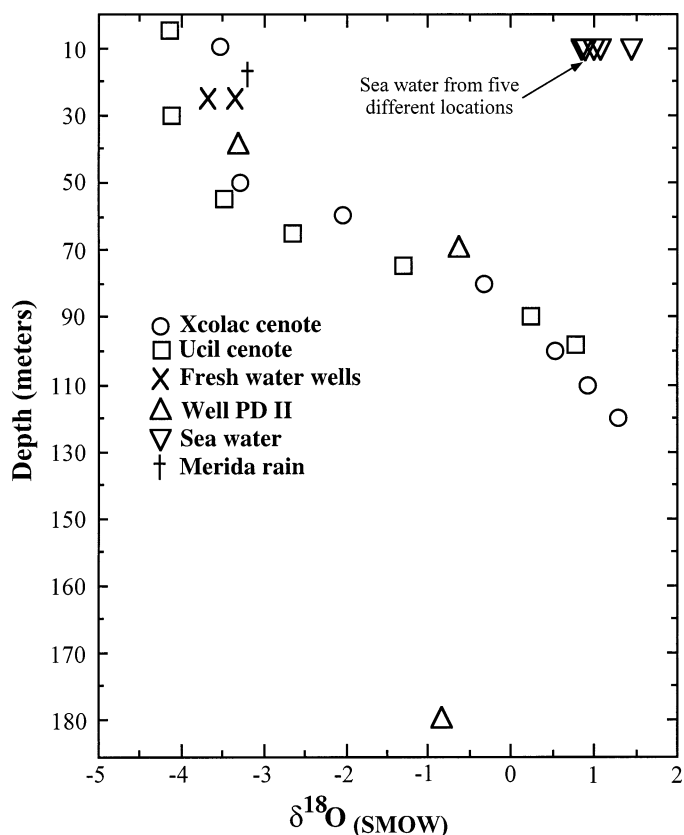


Fig. 5. $\delta^{18}\text{O}$ versus depth for water taken from Xcolac Cenote, Ucil Cenote, two freshwater wells, observation well PD-II, the sea, and rain.

Xcolac Cenotes. This is thus our preferred explanation of low pH waters observed in the lower parts of the water columns of these cenotes.

Surface waters in open cenotes of Yucatan typically have high pH values as a result of evaporation and photosynthetic consumption of CO_2 . At the surface of Xcolac Cenote, the pH is 8.3, whereas at 12 m it drops to 6.8 (Fig. 3). In the water column of partially enclosed Ucil Cenote, the shift in pH of surface water is only a few tenths of a pH unit. A feature present in the Xcolac profile that is absent from the Ucil profile is the slight but definite shift to lower pH between about 10 m and the base of the freshwater lens at 50 m (Fig. 3), with a broad minimum at about 20 m. This might indicate decay of organic matter with consequent CO_2 production. If so, organic substrates might be limiting factors in redox reactions occurring below this zone, especially within the saline intrusion.

Dickman and Thode (1990) studied a vertically stratified water column in a meromictic lake (Crawford Lake, Canada) and found that phototrophic sulfide oxidizing bacteria, specifically *Chromatium* and *Corobium*, tend to migrate to the top of the chemocline. We interpret the shift to low pH in the narrow zone centered on 53 m at Xcolac, labeled as the "sulfide oxidation zone" in Fig. 4, as a zone where sulfide-oxidizing bacteria can exist, as was observed in Crawford lake. Sulfur isotope data, discussed in a subsequent section, also support this interpretation.

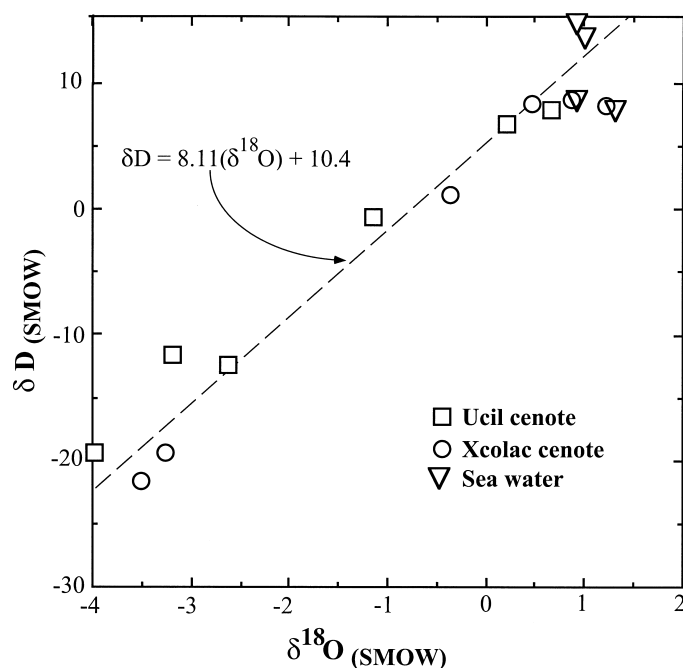


Fig. 6. $\delta^{18}\text{O}$ versus δD . Meteoric precipitation follows a trend defined by the equation $\delta\text{D} = 8.11 \times \delta^{18}\text{O} + 10.4$.

Sulfide concentration, sulfate concentration, and isotope data—The oxygen and deuterium isotope composition of water in Xcolac and Ucil Cenotes confirm their groundwater sources. Above 50 m, water is dominated by meteoric precipitation, with a range in oxygen isotopic composition between about -3‰ and -4‰ (Fig. 5). A sample of local precipitation, taken during a rain storm (Merida Rain), lies within this range at -3.22‰ . A meteoric origin for this freshwater is even more evident when $\delta^{18}\text{O}$ water data are coupled with hydrogen isotope data (Fig. 6). Isotopic values for water above 50 m at Xcolac and above 65 m at Ucil tend to fall along the meteoric water line (here represented by the equation: $\delta\text{D} = 8.11 \times \delta^{18}\text{O} + 10.4$).

Water below 50 m becomes progressively enriched in both ^{18}O and H/D. Oxygen isotope values range from -3.29‰ and -3.48‰ at the base of the freshwater lens in Xcolac and Ucil Cenotes, respectively, to 1.28‰ and 0.78‰ at the bottom of each cenote. Hydrogen isotopes range from -19.7‰ and -12.0‰ at the base of the freshwater lens in Xcolac and Ucil, respectively, to 7.9‰ at 120 m in Xcolac and 7.2‰ at 98 m in Ucil. Well water data show similar trends in $\delta^{18}\text{O}$, ranging from -3.48‰ (average value for two freshwater wells) to -0.62‰ for water taken from 70 m at well PD-II.

The water that is most enriched in oxygen and hydrogen isotopes, occurring at 120 m in Xcolac, is virtually identical in $\delta^{18}\text{O}$ and δD to the average of five different seawater samples collected off the coast at both Progreso, Yucatan, and Isla Mujeres, Quintana Roo (Figs. 5, 6; plotted at 10 m in Fig. 5). These data are consistent with our other observations that groundwater at 120 m depth originated as seawater and has retained its seawater isotopic signature.

Samples of water from deep well PD-II taken below the

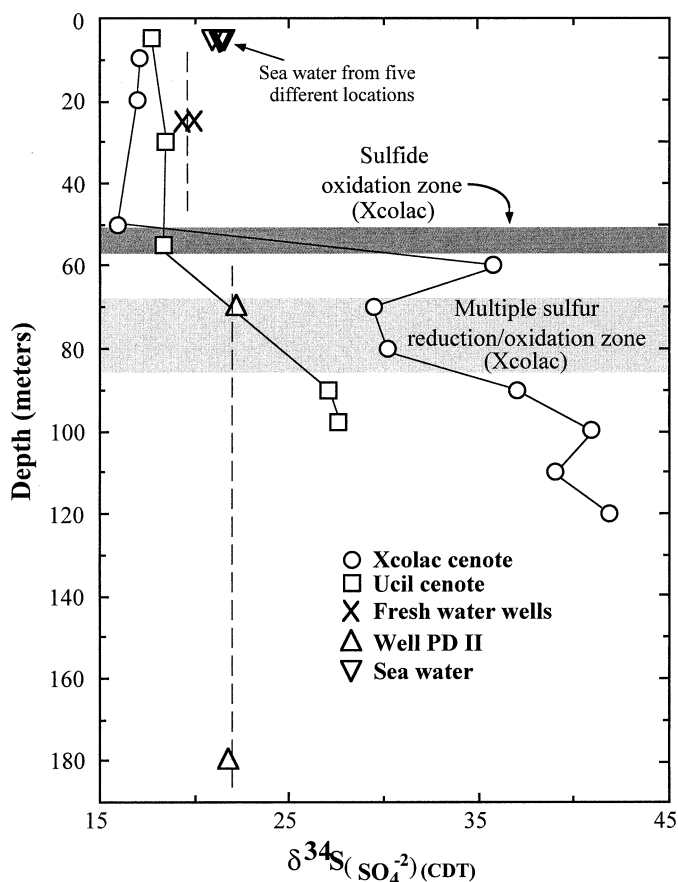


Fig. 7. $\delta^{34}\text{S}$ versus depth of dissolved sulfate from Xcolac Cenote, Ucil Cenote, two fresh water wells, observation well PD-II, and the sea.

saline interface at depths of 70 and 180 m had $\delta^{34}\text{S}$ values of 22.3 and 22.1‰, respectively, very close to the modern marine average value of 21.0‰ (Fig. 7). This is probably typical of the sulfur isotope composition of sulfate of the saline intrusion away from contact with the surface. In contrast, sulfate in the deepest samples from Ucil Cenote were moderately enriched in ^{34}S : $\delta^{34}\text{S}$ at 90 m = 27.1‰ and at 98 m = 27.6‰; that is, they were enriched by 4.9 and 5.4‰ relative to normal values for the saline intrusion. Although sulfide was not analyzed in these samples, they smelled strongly of H_2S when collected, and there is no doubt that bacterial sulfate reduction according to Eq. 1 is the cause of this isotopic shift. At 55 m, which is within the upper well mixed freshwater layer in Ucil, the sulfur isotopic composition of sulfate was 18.3‰, slightly less than the seawater value, and H_2S was undetectable.

The sulfur isotope profiles for Xcolac Cenote are considerably more complicated than Ucil, just as is the case for the pH profile—and for the same reasons. The sharp pH changes recorded by the continuous depth profile between 51 and 55 m in Xcolac water demonstrate the importance of microenvironments within the water column and highlight the possibility of misinterpreting data from our rather widely spaced samples. With that caveat, we note that the $\delta^{34}\text{S}$ of sulfate at 120 m = 41.8‰—20.5‰ enriched in ^{34}S compared to seawater and 14.3‰ enriched compared to the deepest sample from Ucil. There is a more or less regular upward decrease in $\delta^{34}\text{S}$ of sulfate to about 30.2‰ at 80 m, a minimum of 29.5‰ at 70 m, and a sharp spike to 35.8‰ at 60 m (Fig. 7, Table 1). It is thus likely that the 60-m $\delta^{34}\text{S}$ spike (Fig. 7) lies within the zone of increasing pH below the 54-m pH maximum (Fig. 4) and corresponds to an upper zone of sulfate reduction. Sulfate concentration decreases regularly upward from the deepest measurement at 90 m (Fig. 8,

Table 1. Geochemical parameters of Xcolac Cenote waters.

Depth (m)	Conductivity (mS cm^{-1})	$\delta^{18}\text{O}_{\text{water}}$ (‰)		$\delta\text{D}_{\text{water}}$ (‰)	$\delta^{34}\text{S}_{\text{sulfate}}$ (‰)	$\delta^{34}\text{S}_{\text{sulfide}}$ (‰)	SO_4^{2-} (mmol L^{-1})	H_2S (mmol L^{-1})	H_2S (%)	H_2S (mmol L^{-1})	$N_{\text{sulfide}}^\dagger$	$f(\text{S})^\ddagger$ (%)
		Measured	Calculated*									
5	1.18											
10	1.41	-3.53		-21.9	17.1							
20	1.41				17.0							
30	1.41											
40	1.41											
50	1.44	-3.29		-19.7	15.9		81.3	0.85				
55	12				30§	-11.1	128.9	1.3	39.5	1.16	0.46	≤11.0
60	19	-2.04	-2.00		35.8	-17.7	222.2	2.3	42.1	1.24	0.35	17.1
65	25.5		-1.52		34§	-28.2	493.8	5.1	32.4	0.95	0.16	24.3
70	30		-1.09		29.5	-32.2	795.5	8.3	32.2	0.95	0.10	23.2
75	34.7		-0.70		28§	-34§						
80	38.4	-0.32	-0.34	0.8	30.2	-32.9	1051	10.9	51.8	1.52	0.12	22.5
90	45.5		0.24		37.0	-22.5	1288	13.4	134.8	3.96	0.23	23.4
100		0.53	0.66	8.2	40.9	-8.7						
110		0.92	0.92	5.4	39.0	-3.9						
120		1.28		7.9	41.8	-2.5						

* Calculated from the empirical quadratic equation $\delta^{18}\text{O} = -10.84 + 0.196d - 0.00081d^2$, where d = water depth.

$^\dagger N_{\text{sulfate}}$ not tabulated; $N_{\text{sulfate}} = 1 - N_{\text{sulfide}}$.

$^\ddagger f(\text{S}) = N_{\text{sulfide}} \delta^{34}\text{S}_{\text{sulfide}} + N_{\text{sulfate}} \delta^{34}\text{S}_{\text{sulfate}}$.

§ Interpolated value.

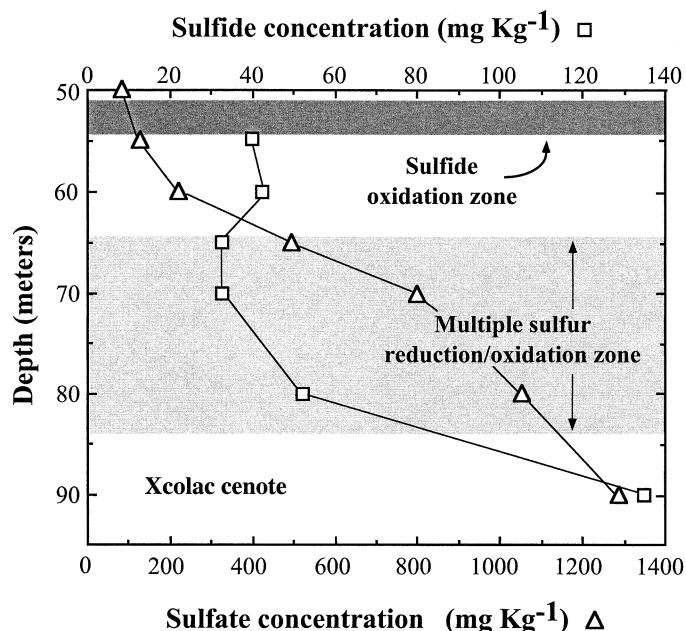


Fig. 8. Sulfate concentration (mg kg^{-1}) and sulfide concentration (mg kg^{-1}) versus depth for water from Xcolac Cenote. These compositional estimates are based on weighing of precipitates collected in the field and are semiquantitative. Sulfate was precipitated by adding 0.5 M BaCl_2 to 1-liter bottles. The presumption is made that all sulfate species precipitate during this treatment. Sulfide was precipitated by adding 0.1 M AgNO_3 to other 1-liter bottles.

Table 1) (13.4 mmol L^{-1} or 47% of the average seawater sulfate concentration [tabulated in Drever 1982]).

These results indicate anaerobic reduction of seawater sulfate by sulfate-reducing bacteria. This bacterially mediated reaction, which involves the reduction of sulfate to sulfide, includes a sequence of enzyme-catalyzed steps that break S–O bonds (Kemp and Thode 1968; Peck 1974). It involves Rayleigh-type processes in which kinetic isotope effects of the form $(k_1/k_2 - 1)1,000$ (‰) occur, where k_1 and k_2 are rate constants for the reduction of the light (k_1) and heavy (k_2) isotopic species.

Stoessel et al. (1993) also noted that sinkholes along the northeastern coast of the Yucatan Peninsula act as local basins for collecting organic material, which in turn is a carbon source for sulfate reduction in those cenotes. The normal seawater $\delta^{34}\text{S}$ values measured in water from the deep well PD-II indicate that redox reactions are important only where the aquifer has an external supply of organic matter, specifically in deep cenotes such as Ucil and Xcolac that penetrate the saline intrusion.

We reiterate that the manner in which we precipitated sulfide does not distinguish between different reduced species. Hence, in this discussion “sulfide” refers to any substance that precipitates as Ag_2S when exposed to a silver nitrate solution. Sulfide concentration is greatest in the deepest samples from Xcolac Cenote, reaches a minimum at about 70 m and then increases slightly in the upper part of the saline intrusion (Fig. 8). (The deepest available concentration measurement is at 90 m.) The ion sum (Table 1): $(m_{\text{sulfate}} + m_{\text{sulfide}})$, where m_{sulfate} and m_{sulfide} are the millimolar concentra-

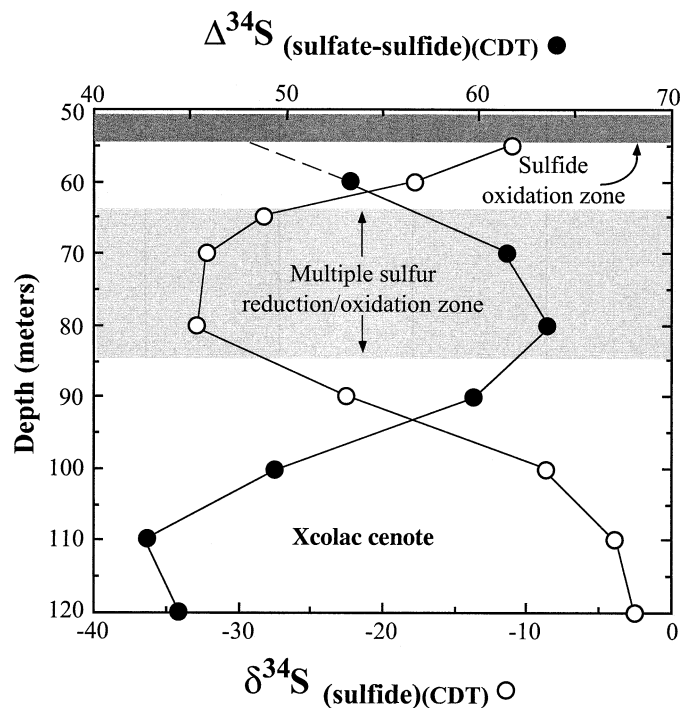


Fig. 9. $\Delta\delta^{34}\text{S}_{\text{sulfate-sulfide}}$ and $\delta^{34}\text{S}_{\text{sulfide}}$ versus depth from Xcolac Cenote.

tions of sulfate and sulfide, respectively, is proportional to conductivity between 60 and 90 m, suggesting that relatively little sulfur is lost from the system. Further support for that statement comes from an isotopic mass balance given below.

Sulfides produced within the Xcolac water column by reactions such as Eqs. 1 and 2 have $\delta^{34}\text{S}$ values ranging from -2.5 ‰ at 120 m to -32.9 ‰ at 80 m (Fig. 9). The difference in the sulfur isotope composition, $\Delta\delta^{34}\text{S}_{\text{sulfate-sulfide}}$, between sulfate and sulfide in the water column of Xcolac Cenote is impressively large, ranging from a minimum of 42.9‰ at 110 m to a maximum of 63.1‰ at 80 m. The latter value is among the largest sulfur isotope difference reported in natural terrestrial systems and appears to represent multiple sulfur reduction/oxidation cycling. Similar but smaller sulfur isotope differences between sulfate and sulfide were observed in Bahamian blue holes (Bottrell et al. 1991), where $\Delta\delta^{34}\text{S}$ between sulfate and sulfide of up to 48.6‰ exist. A few larger values have been reported between sulfides in marine sediments and sulfate in associated pore waters (Canfield and Teske 1996).

It was indicated above that $(m_{\text{sulfate}} + m_{\text{sulfide}})$ is approximately proportional to conductivity. Another indication that sulfur species remain fixed in space, or more likely move at similar rates, comes from a combined mass and isotopic composition balance. In a closed system, if all sulfur comes from the saline intrusion, then $(N_{\text{sulfide}}\delta^{34}\text{S}_{\text{sulfide}} + N_{\text{sulfate}}\delta^{34}\text{S}_{\text{sulfate}}) = 22.2$ ‰, where $N_i\delta^{34}\text{S}_i$ is the mole fraction of species i times the isotopic composition of i (either sulfide or sulfate), and 22.2‰ is the isotopic composition of unmodified aquifer water as found in well PD-II. Values of $(N_{\text{sulfide}}\delta^{34}\text{S}_{\text{sulfide}} + N_{\text{sulfate}}\delta^{34}\text{S}_{\text{sulfate}})$ are tabulated in Table 1 for depths between 55 and 90 m. Between 65 and 90 m, the

calculated values range from 22.5 to 24.3‰ for an average of 23.3‰. Within the limits of our measurements, that is quite close to the predicted closed system value of 22.2‰, with a slight suggestion that sulfide might be migrating out of the system at a rate faster than sulfate. At the top of the saline layer, where sulfide is being converted to sulfate, ($N_{\text{sulfide}} \delta^{34}\text{S}_{\text{sulfide}} + N_{\text{sulfate}} \delta^{34}\text{S}_{\text{sulfate}}$) becomes isotopically depleted in ^{34}S . It is 17‰ at 60 m and ≤ 11 ‰ at 55 m. Furthermore, the sulfate itself at the base of the freshwater lens in Xcolac is depleted in ^{34}S compared to seawater and also compared to sulfate in the freshwater lens in Ucil (Fig. 7). These observations suggest that sulfide is migrating upward somewhat faster than sulfate and that the sulfate at the fresh-/saltwater interface has a component of oxidized sulfide that has selectively moved up in the water column.

The level of sulfate–sulfide $\Delta^{34}\text{S}$ observed in Xcolac at 80 m exceeds the maximum values obtained in laboratory experiments (~ 50 ‰) by Kaplan and Rittenberg (1964). Explaining these large $\Delta^{34}\text{S}$ values requires processes that could include multistep sulfate reduction. Canfield et al. (1998), Habicht et al. (1998), and Canfield (2001) have examined the production of ^{34}S -depleted sulfide within the context of pure laboratory cultures containing sulfate-reducing bacteria. Their results indicate that significant sulfur isotope fractionation (on the order of 40–60‰) occurred when sulfur-disproportionating bacteria were active. Sulfur-disproportionating bacteria tend to grow autotrophically where sulfide concentrations are relatively low and become inactive at sulfide concentrations above 1 mM (Thamdrup et al. 1993). These bacteria disproportionate elemental sulfur to sulfate and sulfide. Habicht and Canfield (2001) further demonstrated that microbial disproportionation was the only known process that could augment observed large sulfur isotope fractionations found in sedimentary sulfides associated with some natural marine systems. Their model shows that sulfide produced during reduction of sulfate is progressively consumed during a series of oxidation reactions to S^0 , SO_3^{2-} , or $\text{S}_2\text{O}_3^{2-}$ and disproportionation to sulfide and sulfate. Although these studies involve reactions taking place in sediments, they appear to be relevant to reactions within the Xcolac water column.

The repeated cycling between sulfide oxidation and subsequent sulfur disproportionation may occur at Xcolac over the depth range in which the greatest sulfur isotope $\Delta^{34}\text{S}$ exists (about 65–80 m). This is shown in Figs. 7–9, where it is labeled the “multiple sulfur reduction/oxidation zone.” The following observations support the conclusion that multiple sulfur reduction/oxidation, sulfur disproportionation, or both processes occur within this zone. There is (1) an overall depletion in the $\delta^{34}\text{S}$ composition of dissolved sulfide between 65 and 80 m with the lightest value occurring at 80 m, (2) a decrease in the concentration of dissolved sulfide relative to the concentration above and below this zone (the greatest decrease in sulfide concentration occurs between 90 and 80 m), and (3) the largest sulfate–sulfide isotope difference ($\Delta[\text{sulfate}–\text{sulfide}]$) within this zone.

As discussed in the section on pH, sulfide oxidation in a narrow band centered on 53 m in Xcolac (sulfide oxidation zone) is probably produced by sulfide-oxidizing bacteria. Immediately below is a zone in which sulfate reduction is

indicated by the minimum in the pH profile (Fig. 4) at 54 m and by a $\delta^{34}\text{S}$ maximum at 60 m, which is perhaps slightly displaced because of depth uncertainty (Fig. 7). Also, sulfide ^{34}S shifts toward more enriched values (-32.2 ‰ at 70 m to -11.1 ‰ at 55 m), which is consistent with sulfate reduction.

Important sulfate reduction zones, as indicated by ^{34}S enrichment of sulfate, occur at the bottom of Xcolac Cenote and just below the freshwater interface. These zones are also characterized by relatively small $\Delta^{34}\text{S}$, which could be related to nutrient supply. Relatively high nutrient availability would be expected in the stagnant saline water layer near the contact with the well-mixed freshwater lens. A zone of relative nutrient enrichment is also present at the bottom of the cenote, where dredge hauls have brought up decaying leaves and branches that fell through the intervening layer.

Parkin and Brock (1980) report that in the presence of a suitable electron donor (H_2S) large population densities of photosynthetic sulfur bacteria typically occur. Takahashi and Ichimura (1970) found that in meromictic or stagnant holomictic lakes, a dense population of phototrophic sulfur bacteria tend to occur in the contact between zones of different oxidation potential. Parkin and Brock (1980) also showed that the rate of oxidation and CO_2 fixation depended on the quality (color) of light penetrating the H_2S zone. They further demonstrated that some strains of photosynthetic sulfur bacteria can survive where light intensities are very low ($<0.4\%$ of the surface intensities). We do not have a quantitative measure of light intensity at 55 m in Xcolac. However, it might be significant that no sharp pH shift is observed near the interface in Ucil where light levels are much lower (Fig. 3).

More recent studies have focused on sulfate reduction in hypersaline marine microbial mats. Canfield and Des Marais (1991) showed that cycling between sulfate reduction and sulfide oxidation occurred in the same zones within the mat depending on the photosynthetic conditions involved. During daylight, photosynthetically derived O_2 dominates the upper portion of the mat (where sunlight penetrates), while sulfide collects below. At night, however, the sulfide layer migrates upward to as high as the surface of the mat–water interface. Canfield and Des Marais (1991) measured the sulfur isotopes of elemental S at the surface of these mats and concluded that the S was derived principally from the dissimilatory sulfate reduction process.

Chemical and isotopic analyses of subsurface waters taken from two deep cenotes, one deep observation well, and two shallow wells in the northern Yucatan peninsula indicate that groundwater in this portion of the peninsula consists of a meteoric freshwater lens that thins toward the coast. Underlying this lens is a saline water layer that extends inland at least 90 km (Perry et al. in press). Water in this intrusion originated as seawater and has retained its seawater isotopic signature.

The isotopic composition of water within the upper 50 m at Xcolac and upper 69 m at Ucil (above the fresh-/saltwater interface) follows the relationship: $\delta\text{D} = 8.11 \times \delta^{18}\text{O} + 10.4$, consistent with a meteoric origin. Water from the underlying saline layer (below the interface) at both cenotes is enriched in ^{18}O and D and is nearly identical in ^{18}O and D composition to seawater collected at the coast to the north.

Furthermore, $\delta^{34}\text{S}$ of sulfate sampled in a deep observation well is also consistent with a seawater origin for this saline layer.

Principal redox reactants in the two deep cenotes (Xcolac and Ucil) are sulfate, which enters from below as a component of the saline water layer, and organic carbon, entering the cenotes as decaying vegetation from the respective drainage basins. Organic matter that does not react in the upper, oxidized layers of the cenotes sinks and is available for redox reactions in the lower saline layer.

Strong $\delta^{34}\text{S}$ enrichment of sulfate from the saline intrusion at both cenotes, contrasts with the seawater value for sulfate from a deep (180 m) observation well. This enrichment in ^{34}S relative to seawater sulfate presumably results from the action of sulfate-reducing bacteria. The large sulfate–sulfide sulfur isotope difference ($\Delta^{34}\text{S} = \sim 63\%$) observed at Xcolac Cenote is consistent with this interpretation and tends to occur in a zone within the water column at Xcolac, indicated by multiple sulfur reduction/oxidation cycling, sulfur disproportionation reactions, or both processes. Both sulfur isotope and pH data indicate that specific processes occur within specific and sometimes narrow depth intervals. Although sulfur isotope measurements at Xcolac come from discrete sample intervals, and thus provide only a rough indication of sulfur isotope zonation within the water column, our pH measurements are continuous and reveal the presence of distinct reaction zones on the order of a few meters thick at a water depth of 53 m (below the fresh-/saltwater interface).

References

- BACK, W., AND B. B. HANSHAW. 1978. Hydrogeochemistry of the northern Yucatan Peninsula, Mexico, with a section on Mayan water practices, p. 93–123. *In* A. E. Weidie [ed.], Guidebook. New Orleans Geological Society.
- BOTTRELL, S. H., P. L. SMART, AND F. WHITAKER. 1991. Geochemistry and isotope systematics of sulfur in the mixing zone of Bahamian blue holes. *Appl. Geochem.* **6**: 97–103.
- CANFIELD, D. E. 2001. Isotope fractionation by natural populations of sulfate-reducing bacteria. *Geochim. Cosmochim. Acta* **65**: 1117–1124.
- , AND D. J. DES MARAIS. 1991. Aerobic sulfate reduction in microbial mats. *Science* **251**: 1471–1473.
- , AND A. TESKE. 1996. Late Proterozoic rise in atmospheric oxygen concentration inferred from phylogenetic and sulfur isotope studies. *Nature* **382**: 127–132.
- , B. THAMDRUP, AND S. FLEISCHER. 1998. Isotope fractionation and sulfur metabolism by pure and enriched cultures of elemental sulfur-disproportionating bacteria. *Limnol. Oceanogr.* **43**: 253–264.
- CRAIG, H. 1957. Isotopic standards for carbon and oxygen and conversion factors for mass spectrometric analysis of carbon dioxide. *Geochim. Cosmochim. Acta* **12**: 133–149.
- DICKMAN, M. D., AND H. G. THODE. 1990. Sulfur bacteria and sulfur isotope fractionation in a meromictic lake near Toronto, Canada, p. 225–241. *In* V. Ihehbot, S. Kempe, W. Michaelis, and A. Spitzg [eds.], Facets of modern biochemistry, Springer-Verlag.
- DREVER, J. J. 1982. The geochemistry of natural waters. Prentice-Hall.
- EPSTEIN, S., AND T. K. MAYEDA. 1953. Variations of ^{18}O content of water from natural sources. *Geochim. Cosmochim. Acta* **4**: 213–224.
- FOSSING, H., AND B. B. JORGENSEN. 1990. Oxidation and reduction of radiolabeled inorganic sulfur compounds in an estuarine sediment, Kysing Fjord, Denmark. *Geochim. Cosmochim. Acta* **54**: 2731–2742.
- FREEZE, R. A., AND J. A. CHERRY. 1979. Groundwater. Prentice-Hall.
- GMITRO, D. A. 1986. The interactions of waters with carbonate rock in Yucatan, Mexico. Unpublished thesis. Northern Illinois Univ., DeKalb.
- HABICHT, K. S., AND D. CANFIELD. 2001. Isotope fractionation by sulfate-reducing natural populations and the isotopic composition of sulfide in marine sediments. *Geology* **29**: 555–558.
- , ———, AND J. RETHMEIER. 1998. Sulfur isotope fractionation during reduction and disproportionation of thiosulfate and sulfide. *Geochim. Cosmochim. Acta* **62**: 2585–2595.
- HILDEBRAND, A. R., G. T. PENFIELD, D. A. KRING, M. PILKINGTON, Z. A. CAMARGO, S. B. JACOBSEN, AND W. V. BOYNTON. 1991. Chicxulub crater: A possible Cretaceous/Tertiary boundary impact crater on the Yucatan peninsula, Mexico. *Geology* **19**: 867–871.
- HOLT, B. D., AND A. G. ENGELKEMEIR. 1970. Thermal decomposition of barium sulfate to sulfur dioxide for mass spectrometric analysis. *Anal. Chem.* **42**: 1451–1453.
- HUT, G. 1987. Report to the Director General. Consultant's group meeting on stable isotope reference standards, Vienna, September 16–18, 1985. International Atomic Energy Agency.
- KAPLAN, I. R., AND S. C. RITTENBERG. 1964. Microbiological fractionation of sulfur isotopes. *J. Gen. Microbiol.* **34**: 195–212.
- KEMP, A. L. W., AND H. G. THODE. 1968. The mechanism of the bacterial reduction of sulphate and of sulphite from isotope fractionation studies. *Geochim. Cosmochim. Acta* **32**: 71–91.
- MARIN, L. 1990. Field investigations and numerical investigations of groundwater flow in the karstic aquifer of Yucatan, Mexico. Unpublished thesis, Northern Illinois Univ., DeKalb.
- PARKIN, T. B., AND T. D. BROCK. 1980. The effects of light quality on the growth of phototropic bacteria in lakes. *Arch. Microbiol.* **125**: 19–27.
- PECK, H. D. 1974. The evolutionary significance of inorganic sulfur metabolism, p. 241–264. *In* M. J. Carlile and J. J. Shekel [eds.], Symposium of the Society for General Microbiology, v. 24.
- PERRY, E., J. SWIFT, J. GAMBOA, A. REEVE, R. SANBORN, L. MARIN, AND M. VILLASUSO. 1989. Geologic and environmental aspects of surface cementation, N. coast, Yucatan, Mexico. *Geology* **17**: 818–821.
- , L. E. MARIN, J. MCCLAIN, AND G. VELAZQUEZ. 1995. Ring of Cenotes “sinkholes”, N.W. Yucatan, Mexico: Its hydrogeologic characteristics and possible association with the Chicxulub impact crater. *Geology* **23**: 17–20.
- , G. VELAZQUEZ-OLIMAN, AND L. MARIN. In press. The hydrogeochemistry of the karst aquifer system of the northern Yucatan Peninsula, Mexico. *Int. Geol. Rev.*
- REBOLLEDO-VIERA, M., J. URUTIA-FUCAGAUCHI, L. E. MARIN, A. TREJO-GARCIA, V. L. SHARPTON, AND A. M. SOLER-ARECHALDE. 2000. UNAM scientific shallow-drilling program of the Chicxulub Impact Crater. *Int. Geol. Rev.* **42**: 928–940.
- SHARPTON, V. L., AND OTHERS. 1993. Chicxulub multiring impact basin: Size and other characteristics derived from gravity analysis. *Science* **261**: 1564–1567.
- SOCKI, R. A. 1984. A chemical and isotopic study of groundwater from Northwestern Yucatan, Mexico. Unpublished thesis, Northern Illinois Univ., DeKalb.
- STERN, L., P. C. BENNETT, AND M. L. PORTER. 2002. Subaqueous and subaerial speleogenesis in a sulfidic cave. *Hydrogeology and*

- biology of post-paleozoic carbonate aquifers, p. 89–91. *In* J. B. Martin, C. M. Wicks, and I. D. Sasowsky [eds.], Proceedings of the Symposium Karst Frontiers: Florida and related environments. Karst Waters Institute Special Publication 7.
- STOESSELL, R. K., Y. H. MOORE, AND J. G. COKE. 1993. The occurrence and effects of sulfate reduction and sulfide oxidation on coastal limestone dissolution in yucatan cenotes. *Ground Water* **31**: 566–575.
- TAKAHASHI, M., AND S. ICHIMURA. 1970. Photosynthetic properties and growth of photosynthetic bacteria in lakes. *Limnol. Oceanogr.* **15**: 929–944.
- THAMDRUP, B., K. FINSTER, J. W. HANSEN, F. AND BACK. 1993. Bacterial disproportionation of elemental sulfur coupled to chemical reduction of iron or manganese. *Appl. Environ. Microbiol.* **59**: 101–108.
- WARD, W. C., G. KELLER, W. STINNESBECK, AND T. ADATTE. 1995. Yucatan subsurface stratigraphy—implications and constraints for the Chicxulub impact. *Geology* **23**: 873–876.
- WEIDIE, A. E. 1985. Geology of the Yucatan Platform. p. 1–19. *In* W. C. Ward et al. [eds.], *Geology and hydrogeology of the Yucatan and Quarternary geology of northeastern Yucatan Peninsula*. NOGS Publications.

Received: 11 September 2001

Amended: 6 June 2002

Accepted: 20 June 2002